ISSN 0965-545X, Polymer Science, Ser. A, 2010, Vol. 52, No. 7, pp. 715–726. © Pleiades Publishing, Ltd., 2010.
Original Russian Text © V.I. Krinichnyi, E.I. Yudanova, N.N. Denisov, 2010, published in Vysokomolekulyarnye Soedineniya, Ser. A, 2010, Vol. 52, No. 7, pp. 1109–1121.

EPR Study of Photoinduced Charge Transfer in a Poly(3-hexylthiophene)–Fullerene Composite[1]

V. I. Krinichnyi, E. I. Yudanova, and N. N. Denisov

Institute of Problems of Chemical Physics, Russian Academy of Sciences, pr. Akademika Semenova 1, Chernogolovka, Moscow oblast, 142432 Russia
e-mail: yudan@icp.ac.ru

Received July 16, 2009;
Revised Manuscript Received October 13, 2009

Abstract—Magnetic, relaxation, and dynamic parameters of radical pairs of positively charged polarons and negatively charged anion radicals of fullerene that are induced by photons with an energy of 1.7–3.4 eV are studied by the methods of photoinduced electron paramagnetic resonance for the poly(3-hexylthiophene)–fullerene composite. The above charge carriers show mutual independence, which is provided by a different interaction with their microenvironment. The paramagnetic susceptibility of spin pairs reflects the dipole–dipole interaction and activation dynamics of paramagnetic sites in the polymer–fullerene system. The rate of recombination of radical pairs is controlled by the mutual space distribution of carriers of various charges and by the energy of excitation photons. Quasi-one-dimensional diffusion of polarons along polymer chains and rotational diffusion of fullerene molecules about the selected molecular axis are likewise controlled by the energy of photons and can be described in terms of the activation Elliott hopping model. The dependence of the main values of magnetic, relaxation, and dynamic parameters of charge carriers on the energy of photons is explained by the inhomogeneous distribution of molecular clusters in the polymer–fullerene composite. The annealing of this composite leads to an enhanced formation of polymer crystallites and fullerene clusters. Hence, the effective dimension of the system increases and its electron characteristics are improved.

DOI: 10.1134/S0965545X10070060

INTRODUCTION

In the last two decades, numerous studies have been devoted to the synthesis and characterization of properties of polymers with continuous π-electron delocalization. These compounds can be used in molecular electronics as the most promising materials for polymer photovoltaic applications, and, currently, intensive development of this direction is responsible for their comprehensive investigation [1, 2]. The most effective components for the development of plastic solar cells are soluble conjugated polymers and fullerene derivatives [3, 4]. Fullerene molecules in the matrix of a conjugated polymer interact with its macromolecules and form a so-called bulk heterojunction; they serve as electron donors and acceptors in plastic solar batteries. Polymer and fullerene molecules have different affinities toward electrons; hence, in the formed bulk heterojunction, photogeneration and separation of charge carriers occur during illumination. In this case, positive charges are transferred by polarons that diffuse in the polymer, whereas electrons are transferred by hopping between contacting domains of fullerenes according to the hopping mechanism. The evident advantages of the above bulk heterotranstions are their easy preparation via the dissolution of initial components in organic compounds and the subsequent casting of the prepared solution onto a rotating support. At the present time, the efficacy of solar cells with bulk heterojunction is 5–6% [2]. This parameter is controlled by the energy of polaron binding and by the density and mobility of charge carriers in organic solar cells, which are smaller than their classical crystalline analogs. In polymer–fullerene systems, it is possible to distinguish short-living pairs, which recombine immediately once the light is switched off, as well as charge carriers with longer lifetimes [5, 6]. For short-living pairs, the recombination depends on the intensity of excitation light and can be described in terms of the activation bimolecular process [7]. For long-living pairs, the kinetics of recombination is independent of the intensity of initiating light and is controlled by the presence of entrapped carriers in the system owing to the system's structural heterogeneity [5]. Long-living charge carriers are formed by localized polarons, which are entrapped by traps with an energy exceeding kT. Their recombination can be explained by nongeminate collisions of randomly distributed charges. The mechanism of recombination is controlled by tunneling processes, while the recombination rate is controlled by the distances between photoexcited charges. It is evident that the molecular features in the structure of the

[1] This work was supported by the Russian Foundation for Basic Research, 08-03-00133, and by the Human Capital Foundation, project no. 27-02-5.

polymer–fullerene system should control the rate and mechanism of photoexcitation of charge carriers in this system as well as their separation and recombination. Therefore, analysis of the electron processes happening in such systems not only is crucial from the fundamental viewpoint but also is of practical interest for the search for new optimum materials to be used in photovoltaics. However, so far, the mechanism of the main processes in plastic solar cells remains vague.

Photoinduced charge transfer is accompanied by the formation of a radical pair, $P^{+\bullet}-C_{60}^{-\bullet}$, of paramagnetic sites with spins $S = 1/2$; hence, their relaxation and dynamic characteristics can be studied by the direct method of light-induced EPR (LEPR) [8, 9]. In the LEPR spectra, two overlapping EPR signals are seen; these signals have different band lengths and amplitudes, and their saturation with an increase in the microwave field is likewise different. As was shown earlier [10–12], the main magnetic, relaxation, and dynamic parameters of charge carriers photoinduced in the polymer–fullerene system depend on the energy of absorbed photons. In addition, it was found [13, 14] that, among soluble fullerene derivatives with different structures of side alkyl substituents, the most promising electron acceptor for plastic solar cells is 6,6-phenyl-C_{61}-butyric acid methyl ester (PCBM). In the bulk heterojunction, the mobility and lifetime of charge carriers are markedly increased when poly(3-hexylthiophene) (PHT) is used as a polymer matrix [15]. The combination of the best, relative to other organic polymers, structural ordering of PHT and the specific morphology of the bulk heterojunction of the PHT–PCBM system is likely to provide a higher screening of the Coulomb potential of interaction between radical pairs photoinduced in a given system. As a result of this interaction, the interaction between them becomes weaker, their separation becomes more effective, and the probability of further recombination decreases. The above features make it possible to increase the high efficacy of solar-energy conversion of plastic solar cells. In this context, the PHT–PCBM composite has been selected as a model system for studying the photoinduction of radical pairs and their further recombination in the bulk polymer–fullerene heterojunction.

This article presents pioneering results of the study of magnetic, relaxation, and dynamic parameters of polarons and anion fullerene radicals induced in the bulk PHT–PCBM heterojunction by photons with an energy of 1.7–3.4 eV in a broad (77–300 K) temperature interval via the method of LEPR spectroscopy. It is shown that, in the radical pair, charge carriers weakly affect each other and, hence, they differently interact with their microenvironment. This approach makes it possible to separately estimate magnetic and relaxation parameters of both types of charge carriers and to consider their dynamics in the bulk PHT–PCBM heterojunction. The effect of the energy of initiating photons on the main electron characteristics of the system that is induced by the inhomogeneous distribution of molecular clusters in the system is presented. The effect of annealing on the electron characteristics of an organic solar cell is analyzed.

EXPERIMENTAL

In this study, regioregular PHT (Rieke Metals, United States) and PCBM (Solenne BV, Netherlands) were used. These components at a weight ratio of 1 : 1 were dissolved in chlorobenzene until the concentration was 1 wt %. The prepared solution was cast as a thin layer on a ceramic plate and dried; as a result, a film with dimensions of 4 mm × 8 mm and a thickness of ~0.1 mm was formed. In addition, a similar sample that was annealed in an inert atmosphere at 413 K for 1 h was used.

The EPR spectra were recorded with a 3-cm PS-100X computer-aided spectrometer (9.7 GHz); the modulation frequency of the constant magnetic field was 100 kHz. The magnetic component of microwave field B_1 in the center of the resonator was estimated from the analysis of broadening of the EPR spectrum of a single crystal of diphenylpicrylhydrazine according to a well-known procedure [16]. Dark-field and light-induced EPR spectra of the initial PHT and the PHT–PCBM composite were recorded at 90–340 K with a BRT temperature unit (Special Design Bureau, Institute of Organic Chemistry, Russian Academy of Sciences) and at 77 K with the use of a Dewar flask filled with liquid nitrogen. Photoinduction of radical pairs in the PHT–PCBM sample was performed directly in the microwave resonator of the EPR spectrometer through the use of a DM-4T source equipped with a KGM 12-100-5 halogen lamp. The energy of photons was changed with the use of a relevant set of glass light filters. The signal—noise factor of the EPR spectra was increased according to the procedure of signal accumulation under repeated (6–20 times) scanning of the spectrum. Paramagnetic susceptibility was estimated by double integration of the corresponding EPR spectra recorded at identical experimental conditions. The EPR spectra were modeled according to the WinEPR SimFonia program (Bruker). The maximum error in measurements and simulation of the width of EPR band, δ, was ±2 μT. Optical absorption spectra of the samples and transmittance spectra of light filters were recorded on a Shimadzu UV-3101PC scanning spectrophotometer at room temperature.

RESULTS AND DISCUSSION

Magnetic Resonance Parameters

EPR line shape and *g* factor. In the absence of illumination, PHT and PCBM show no EPR spectra over the entire temperature interval. When the PHT–PCBM system is illuminated with visible light directly

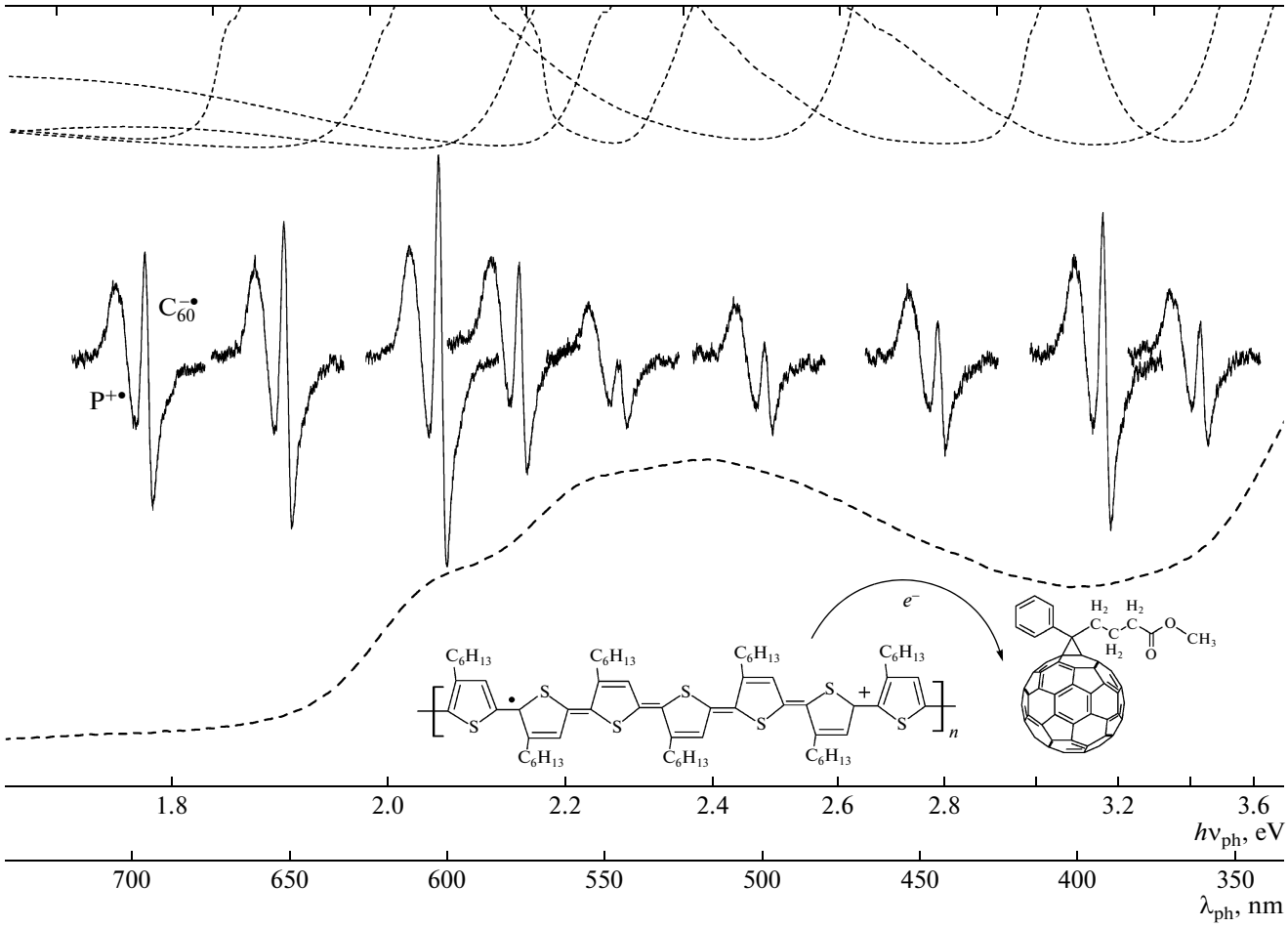

Fig. 1. LEPR spectra of $P^{+\bullet}$–$C_{60}^{-\bullet}$ radical pairs photoinduced in the PHT–PCBM system at 77 K by light photons with energy $h\nu_{ph}$ (λ_{ph} is the wavelength). The left-hand EPR spectrum shows the lines corresponding to charge carriers $P^{+\bullet}$ and $C_{60}^{-\bullet}$. Dashed lines show the (upper spectra) optical transmittance spectra of the corresponding filters and (lower spectrum) absorption spectrum for the PHT–PCBM system. The lower images show the structure of the PHT macromolecule, on which a mobile polaron is formed, and PCBM.

in the resonator of the EPR spectrometer at $T \leq 200$ K, two overlapping LEPR lines are seen; the ratio between their intensities is temperature-dependent. Figure 1 shows the LEPR spectra for the radical pair formed by positively charged polaron $P^{+\bullet}$ with an effective g factor ($g_1 = 2.0012$) and negatively charged anion radical $C_{60}^{-\bullet}$ with an effective g factor ($g_2 = 1.9996$) induced in the PHT–PCBM system under the action of photons with different energy $h\nu_{ph}$. For comparison, Fig. 1 presents the optical absorption spectrum for the PHT–PCBM system and the transmittance spectra of light filters.

The effective EPR spectrum is controlled by the forbidden structure of individual lines, which are related to nonsymmetric orbital interaction of each of the spins of charged particles in the molecular system. In this π-conjugated electron system, deviation of the g factor of the polaron from the g factor of a free electron ($g_e = 2.0023$) is provided by the noncompensated orbital moment, which induces an additional magnetic field under the consecutive excitation $\sigma \rightarrow \pi \rightarrow \sigma^*$. In this case, this deviation Δg should depend on the constant of spin–orbit interaction, λ, and on the difference in energies between levels σ and π, $\Delta E_{\sigma\pi}$ and between levels π and σ*, $\Delta E_{\pi\sigma^*}$ [17]:

$$\Delta g = -\frac{\lambda}{3}\left(\Delta E_{\sigma\pi}^{-1} - \Delta E_{\pi\sigma^*}^{-1}\right) \quad (1)$$

Because of π-π* direct excitation, the orbital moment is negligibly small and manifests itself only for the nearest carbon atoms. In contrast, the anisotropy of the g factor can be provided by additional fields along axes x and y, which are directed along the σ plane of the molecular polymer backbone. Indeed, study of poly(3-octylthiophene) and its close structure by the method of 2-mm EPR spectroscopy showed [17] that the interaction of an unpaired electron (delo-

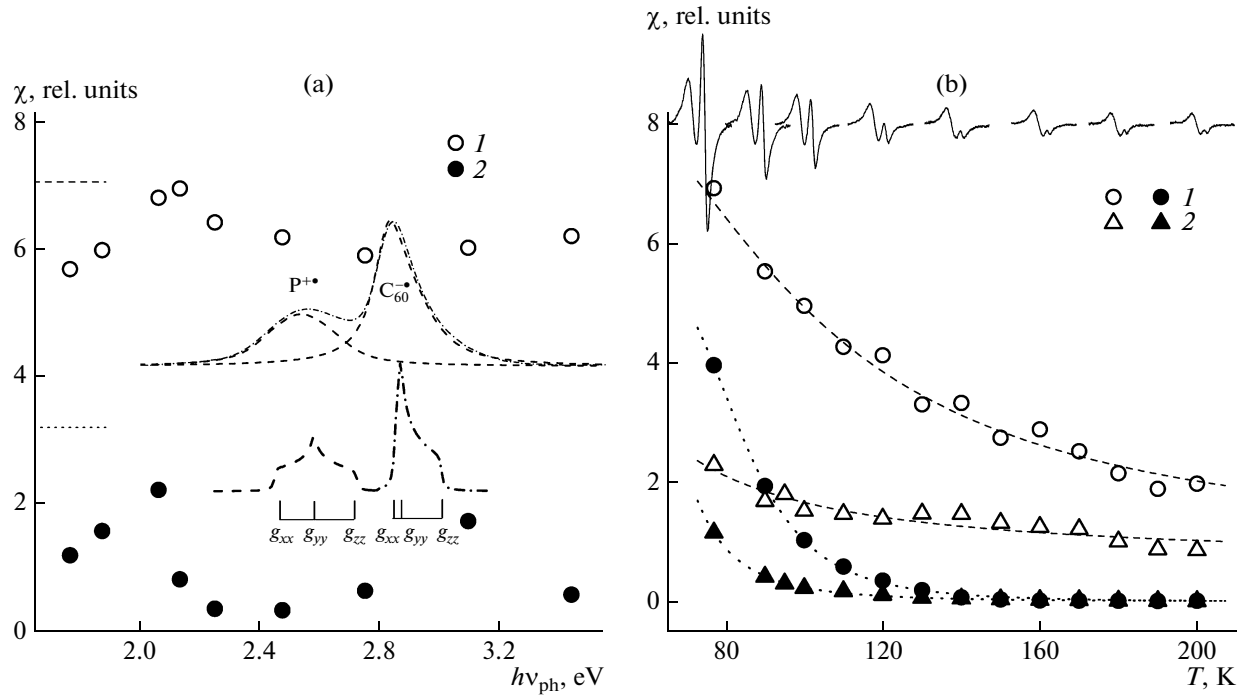

Fig. 2. (a) Paramagnetic susceptibility χ of (*1*) polarons $P^{+\bullet}$ and (*2*) fullerene anion radicals $C_{60}^{-\bullet}$ at 77 K in the initial composite plotted against the energy of photons of incident light, $h\nu_{ph}$. Parameters estimated for charge carriers during illumination with white light at 77 K are shown as fragments of dashed and dotted lines, respectively. The integral LEPR spectrum is presented as the sum of the spectra of both charge carriers with the corresponding anisotropic g_{ii} factors. (b) Temperature dependences of paramagnetic susceptibility χ estimated for (open circles) $P^{+\bullet}$ and (closed circles) $C_{60}^{-\bullet}$ that are photoinitiated by illumination with white light for (*1*) initial and (*2*) annealed PHT–PCBM samples after annealing for 1 h at 413 K. Dashed and dotted lines show the dependences calculated through Eq. (5) for tabulated ΔE_{ij} values. The upper LEPR spectra correspond to the radical pairs recorded at the corresponding temperatures and under identical experimental conditions.

calized on a polaron) with a sulfur heteroatom included in the polymer structure leads to the anisotropy of its *g* factor: $g_{xx} = 2.00409$, $g_{yy} = 2.00332$, and $g_{zz} = 2.00235$. For a fullerene anion radical induced in the PHT–PCBM composite, the effective *g* factor is typical of other fullerene anion radicals [18]. As in the case of the initial fullerene molecule C_{60} [19], the difference between the *g* factor of a PCBM ion radical and g_e is related to the fact that orbital angular moment of stabilized spin is not fully retarded. The formation of the $C_{60}^{-\bullet}$ anion radical changes the isotropic icosahedral symmetry of the initial fullerene molecule owing to the dynamic Jahn–Teller effect and its structural deformation [20].

Paramagnetic susceptibility. Figure 2 presents relative spin susceptibility χ of polarons and fullerene anion radicals in the PHT–PCBM system estimated by double integration of the LEPR signals, depending on the energy of initiating photons and temperature. This evidence shows that the number of polarons $P^{+\bullet}$ is several times higher than the number of fullerene $C_{60}^{-\bullet}$ anion radicals in all intervals of variations in photon energy and temperature. Note that, in the experiments, the steady-state concentration is recorded; this concentration includes the processes of generation ad recombination of spins. It is possible that an excess of polaron spins in the polymer is provided by light-induced excitons, which break down into pairs of positively and negatively charged polarons, or by the development of additional spin excitations, which do not lead to emergence of a charge, for example, solitons. Some polarons are localized in the amorphous polymer phase or on defects and can be repeatedly excited under the action of temperature. As was shown earlier [10–12], the shape of the LEPR line in the poly(3-dodecylthiophene)–PCBM system depends on initiating-photon energy $h\nu_{ph}$. A similar pattern is observed for the composite under study. Figure 2a shows that, at a fixed temperature, an increase in $h\nu_{ph}$ leads to changes in the relative concentrations of both charge carriers in the PHT–PCBM composite with extrema at $h\nu_{ph} \approx 2.0$ and 3.1 eV.

The interaction and dynamics of paramagnetic sites of radical pairs can be noticeably changed via thermal annealing of the composite. Figure 2b shows the temperature-induced changes in the shape and intensity of the LEPR spectrum as well as paramag-

ΔE_{ij}, E_a, E_{ph}, and E_b estimated through Eqs. (5), (6), (13), and (14) for radical pairs photoinduced by illumination with white light for the initial and annealed (1 h, 413 K) PHT–PCBM samples

Sample	Radical	ΔE_{ij}, eV	E_a, eV	E_{ph}, eV	E_b, eV
Initial	$P^{+\bullet}$	0.012	0.015	0.034	–
	$C_{60}^{-\bullet}$	0.042	–	–	0.032
Annealed	$P^{+\bullet}$	0.008	0.017	0.021	–
	$C_{60}^{-\bullet}$	0.045	–	–	0.007

netic susceptibility of polaron χ_P and fullerene anion radical χ_C of initial and annealed PHT–PCBM samples. As follows from Fig. 2b, in the low-temperature interval, the initial PHT–PCBM sample is characterized by a stronger decay of the temperature dependence of χ_C than that of the corresponding dependence of paramagnetic susceptibility χ_P. As a result of annealing of the sample, both values become less dependent on temperature, and their ratio slightly changes. This effect can be explained as follows. Let us assume that a positively charged polaron diffuses along the polymer chain from unit i to another unit j, which is located near a negatively charged fullerene molecule. Hops of charges between fullerene molecules proceed more easily than charge hops between polaron and fullerene; hence, the effective recombination of charges is primarily limited by the rate of polaron transfer to fullerene molecules. With allowance for the high anisotropy of the dynamics of polarons in undoped and slightly doped conjugated polymers [17–21], it is possible to assume that the probability of charge transfer along the polymer PHT chain markedly exceeds the probability of charge transfer between neighboring macromolecules. Once the polaron and the fullerene approach each other, charge recombination primarily proceeds via tunneling of an electron from fullerene onto the polaron with a characteristic time [23]:

$$\tau(R'_{ij}) = \tau^0_{pn}\exp\left(\frac{2R'_{ij}}{a_0}\right), \quad (2)$$

where τ^0_{pn} is a constant, R'_{ij} is the distance between units i and j, and a_0 is the radius of effective charge localization (the Bohr radius). Charge transfer along the polymer chain is provided by polarons via tunneling through the energy barrier $\Delta E_{ij} = E_j - E_i$ within time t [23]:

$$\tau(R_{ij}, E_{ij}) = \tau^0_{pp}\exp\left(\frac{2R_{ij}}{a_0}\right)\exp\left(\frac{\Delta E_{ij}}{k_B T}\right), \quad (3)$$

where τ^0_{pp} is a constant, k_B is the Boltzmann constant, and T is the temperature. Two mechanisms of charge transfer are the main cause of the fact that the decrease in paramagnetic susceptibility of positively charged polarons in the regioregular PHT includes two contributions: a fast and temperature-independent contribution and a slow contribution, which exponentially changes with temperature [6]. Moreover, it is necessary to consider quasi-one-dimensional (1D) motion of a polaron, which affects the dipole–dipole interaction between two types of charges and, hence, their paramagnetic susceptibility. When 1D hops from region i to region j with frequency ω_h, a positively charged polaron can collide with a fullerene anion radical, which is located near polymer chain. In contrast to a polaron with translational movement along polymer chain, fullerene molecules rotate about a given molecular axis without any changes in its space position. In this case, the probability of rotation of spins, p, during their collision should depend on the strength of bulk interaction and ω_h [24]:

$$p = \frac{1}{2}\frac{\alpha^2}{1+\alpha^2}, \quad (4)$$

where $\alpha = 3\pi J/\hbar\omega_h$, $\hbar = h/2\pi$ is Planck's constant, and J is the constant of bulk spin interaction. Depending on the intensity of interaction, an increase in ω_h can lead to either a decrease or an increase in the exchange frequency. With allowance for the direct dependence of the steady-state concentration of paramagnetic sites on their lifetime, Eqs. (2), (3), and (4) give the final expression for the paramagnetic susceptibility of the polymer–fullerene system:

$$\chi_p = \chi_{pn} + \chi^0_P\frac{\hbar}{J}\left(\alpha + \frac{1}{\alpha}\right) \quad (5)$$

Assuming the activation character of 1D translational diffusion of a polaron with frequency $\omega_h = \omega^0_h\exp(-\Delta E_{ij}/k_B T)$ (here, ΔE_{ij} is the activation energy), we simulate the temperature dependences of spin susceptibilities, $\chi(T)$, of a polaron and a fullerene anion radical according to Eq. (5) for conventional and annealed samples. The best fit is observed at J = 0.2–0.35 eV, and ΔE_{ij} is listed in the table. Figure 2b shows the calculated curves. As follows from the table, ΔE_{ij} estimated for polarons photoinduced by white light in the PHT–PCBM composite decreases after annealing. Hence, it may be concluded that, in the annealed sample, the dynamics of polarons is activated at a comparatively lower energy than that in the

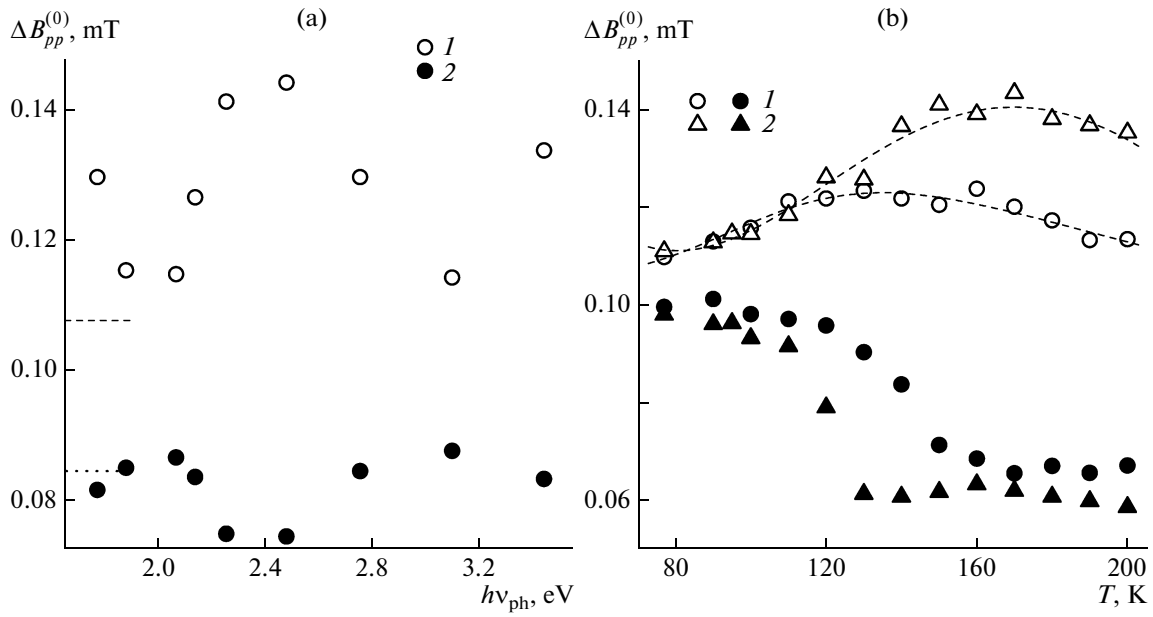

Fig. 3. (a) LEPR linewidth $\Delta B_{pp}^{(0)}$ of (*1*) polarons $P^{+\bullet}$ and (*2*) fullerene anion radicals $C_{60}^{-\bullet}$ during continuous illumination of the PHT–PCBM composite at 77 K by photons with different energy $h\nu_{ph}$ plotted against the energy of photons of incident light, $h\nu_{ph}$. Fragments of dashed and dotted lines show the corresponding $\Delta B_{pp}^{(0)}$ values for the composite illuminated with white light at 77 K. (b) Temperature dependences of $\Delta B_{pp}^{(0)}$ for (open circles) polarons $P^{+\bullet}$ and (closed circles) fullerene anion radicals $C_{60}^{-\bullet}$ during illumination with white light for (*1*) initial and (*2*) annealed PHT–PCBM samples. Dashed lines show theoretical dependences calculated through Eq. (6) for tabulated E_a values.

initial sample, an effect that is likely provided by the lower structural inhomogeneity of the initial polymer matrix due to annealing. Analysis shows that constant J changes in the range from 0.2 to 0.35 eV. This value is markedly higher than the corresponding radical of spin exchange of nitroxyl radicals with paramagnetic ions in liquids, $J \le 0.01$ eV [25], but it lies near $J \approx 0.36$ eV, which was obtained for the interaction of polarons with oxygen molecules in doped polyaniline [26, 27].

The peak-to-peak linewidth. Figure 3 presents the effective peak-to-peak linewidth $\Delta B_{pp}^{(0)}$ plotted against the energy of photons and the temperature for radicals $P^{+\bullet}$ and $C_{60}^{-\bullet}$ in the absence of microwave saturation. The $\Delta B_{pp}^{(0)}$ is shown to change with $h\nu_{ph}$ nonmonotonically and shows extrema at 2.0 and 3.1 eV (Fig. 3a). The first extremum is located in the vicinity of the energy gap of PHT, $E_g = 1.92$ eV [28], whereas the nature of the second extremum can be related to the existence of clusters with different structural ordering in the sample.

Temperature dependences of the linewidth of polarons photoinduced in the initial and annealed PHT–PCBM samples pass extrema at 140 and 170 K (Fig. 3b). Extrapolation to the high-temperature region gives $\Delta B_{pp}^{(0)} = 0.09$ mT at room temperature, a value close to the values that were earlier obtained for polarons stabilized in the matrices of the PHT–PCBM [13, 14] and poly(3-dodecylthiophene)–PCBM composites [10–12]. This value is appreciably lower than the linewidth of polarons stabilized in undoped polythiophene [29], a result that can be explained by a lower spin interaction in the system under study. If we assume that the interaction of a fullerene anion radical with polarons has an activation nature and that diffusion of a polaron proceeds according to the hopping mechanism along the polymer chain at rate $\omega_h = \omega_h^0 \exp(-\Delta E_{ij}/k_B T)$ and activation energy E_a, the dependences shown in Fig. 3b can be described in terms of the above exchange dipole–dipole interaction of two spins. According to this theory, collisions of spins should lead to an additional broadening of the LEPR band by the value [24]

$$\delta(\Delta\omega) = p\omega_h C = \frac{\pi}{3} C \frac{J}{\hbar}\left(\frac{\alpha}{1+\alpha^2}\right), \qquad (6)$$

where p is the probability given by Eqs. (4) and C is the number of paramagnetic sites per monomer of the polymer matrix.

Figure 3b shows the temperature dependences of the linewidth, $\Delta B_{pp}^{(0)}(T)$, calculated through Eq. (6) with the use of the tabulated E_a values (dashed lines). Analysis of the above evidence shows that activation

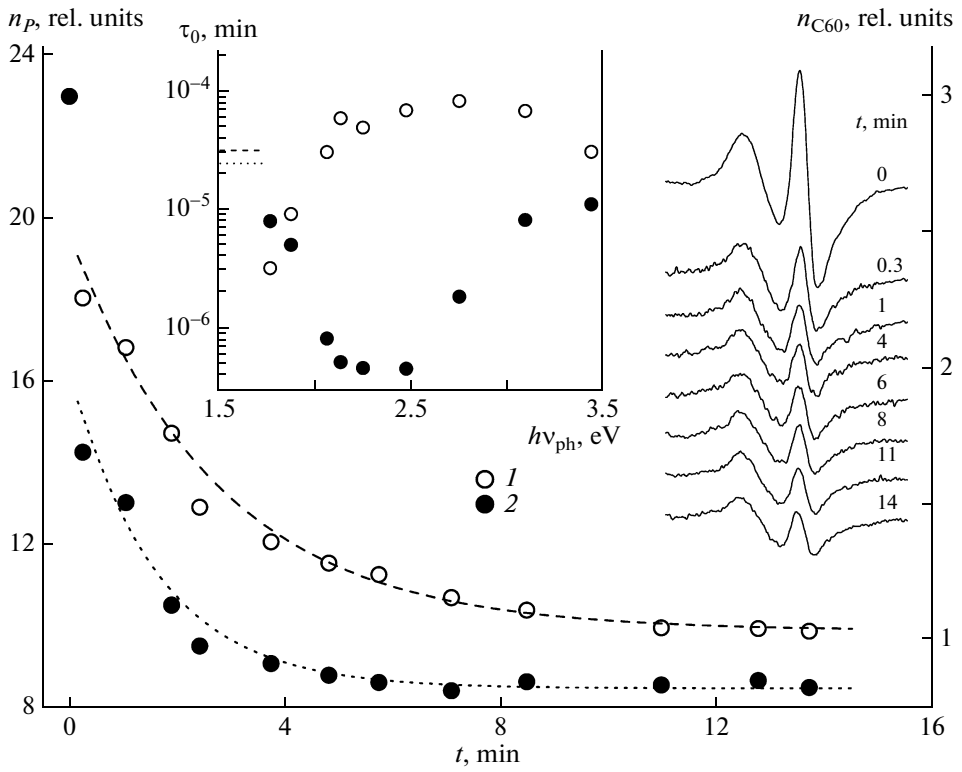

Fig. 4. Typical dependences of changes in (*1*) concentration of polarons $P^{+\bullet}$ n_p, and (*2*) fullerene anion radicals $C_{60}^{-\bullet}$, n_{C60} at the blackout instant at $T = 77$ K. Dashed and dotted lines show the dependences calculated through Eq. (10). In the right-hand part, changes in the profile and intensity of integral LEPR spectrum of the composite at the instant of blackout of initiating light are shown. The central insert shows the dependence of lifetime τ_0 of photoexcited charge carriers (*1*) $P^{+\bullet}$ and (*2*) $C_{60}^{-\bullet}$ on the energy of photons, $h\nu_{ph}$. The corresponding values estimated for the above charge carriers photoexcited in the sample during continuous illumination with white light are indicated with fragments of dashed and dotted lines.

energy E_a for the annealed PHT–PCBM composite differs only slightly from that of the initial sample.

This evidence makes it possible to conclude that the main magnetic-resonance parameters of both types of charge carriers depend on the energy of initiating photons. The formation of charge carriers with different characteristics in the homogeneous regions of the composite may be expected, and this formation can be provided by the presence of photoinitiated traps with different depths in the polymer matrix. Both of the identical charge carriers are formed in the heterogeneous regions of this system. This dependence of the parameters of paramagnetic sites on the frequency of initiating radiation is likely provided by their interaction with the microenvironment in the molecular clusters, which are nonuniformly distributed in the polymer–fullerene system. Different ordering of such clusters may be responsible for the scatter in the band-gap energy, a circumstance that should lead to their susceptibility toward quanta with different energies. This factor can be used for the preparation of photovoltaic devices with controlled characteristics.

Recombination of Charge Carriers

In solar cells, the transfer of positive and negative charges proceeds via the diffusion of carriers to electrodes under the action of an electric field so that charges initiated by photon should approach electrodes; hence, passage time t_{tr} should be appreciably lower than the lifetime of a radical pair, τ ($t_{tr} \ll \tau$). Once the incident light is switched off, the concentration of spin pairs starts to decrease at a high rate. Figure 4 shows typical curves illustrating the decay of the concentration of spin carriers photoinitiated in the PHT–PCBM composite at 77 K. In addition, Fig. 4 shows the dynamics of changes in the intensity and profiles of the LEPR spectra after the blackout. The rate of recombination of charges with effective localization radius a and spacing distance R can be written as follows [30]:

$$\nu(R) = \nu_0 \exp\left(-\frac{2R}{a}\right), \quad (7)$$

where ν_0 is a constant. In the calculations, it is necessary to consider the difference in localization radii a of charge carriers. For an electron, this radius may be assumed to be nearly equal to the radius of the mole-

cule of modified PCBM fullerene, which is controlled by the structure of its side alkyl substituent [31]. In the conjugated polymers, the length of a polaron is usually five monomer units [6, 32]. The distance between the nearest charge carriers, $R(t)$, changes with time as

$$R(t) = \frac{a}{2}\ln\left(\frac{t}{\tau_0}\right) \quad (8)$$

When the initial concentration of charge carriers at the instant of blackout at time $t_0 = 0$ is denoted as n_0 and $t_1 - t_0$ is the time of charge recombination, it is possible to write the following expression illustrating changes in the concentration of spins with time [30]:

$$n(R) = \frac{n}{1 + \frac{4\pi}{3}n_1\left(R^3 - R_1^3\right)}, \quad (9)$$

where R is defined by Eq. (8), $R_1 = R(t_1)$ is the distance between the nearest charge carriers at time t_1 at the instant of their recombination, and n_1 is the concentration of charge carriers at time t_1. As follows from Eq. (9), the residual concentration of charges decreases with time not through an exponential dependence but through a less steep logarithmic dependence. By extrapolation $t \longrightarrow \infty$ (or at high R), we have $n(R) = [(4\pi/3)R^3]^{-1}$, which is independent of the concentration of n_1 and n_0. As follows from Eq. (7), photoexcited charges are characterized by comparatively high lifetimes, a behavior that is primarily provided by an increase distance between drifting charge carriers of the same radical pair. The concentration of spins is estimated directly from the LEPR spectra, and localization radius a and typical lifetime $\tau_0 = \nu_0^{-1}$ can be estimated from general physical speculations. The final equation for the kinetics of termination of radical pairs can be written as follows [30]:

$$\frac{n(t)}{n_0} = \frac{\frac{n_1}{n_0}}{1 + \left(\frac{n_1}{n_0}\right)\frac{\pi}{6}n_0a^3\left[\ln^3\left(\frac{t}{\tau_0}\right) - \ln^3\left(\frac{t_1}{\tau_0}\right)\right]} \quad (10)$$

In addition, Fig. 4 presents the dependences calculated through Eq. (10). Dashed and dotted lines show the dependences (calculated through Eq. (10)) with $n_0a^3 = 2.21 \times 10^{-4}$ and $\tau_0 = 7.2 \times 10^{-5}$ min and with $n_0a^3 = 1.4 \times 10^{-3}$ and $\tau_0 = 3.6 \times 10^{-7}$ min, respectively. As follows from Fig. 4, experimental data can be well approximated by the above equation. The analysis shows that the concentration of photoexcited spin pairs at time $t = 0$ is controlled by several factors, including energy of photons $h\nu_{ph}$. The insert in Fig. 4 shows changes in the typical lifetime of polarons and fullerene anion radicals, τ_0 (Eq. (10)) with varying energy of photons $h\nu_{ph}$. Dashed and dotted lines show the value estimated for the above carriers, which are photoexcited in the sample by continuous irradiation with white light. This evidence suggests quite opposite changes in this value as a function of $h\nu_{ph}$. Product n_0a^3 and the lifetime calculated for both types of charge carriers are close to $n_0a^3 \sim 10^{-3}$ and $\tau_0 \sim 10^{-6}$ min estimated in [30] for the bulk heterojunction of PCBM with macromolecules of another polymer matrix. Therefore, the kinetics of termination of long-living spin pairs photoexcited in the PHT–PCBM composite and similar composites can actually be interpreted in terms of the above model, which relates the recombination rate to the spactial separation of photoinitiated charges.

Electron Relaxation and Dynamics of Charge Carriers

When the intensity of the microwave field is increased, LEPR spectra broaden and their intensities nonlinearly increase. The above changes in the LEPR spectra are provided by the effect of continuous saturation of paramagnetic sites. Analysis shows that saturation of the LEPR spectra of polarons and fullerene anion radicals occurs at different microwave intensities. This fact makes it possible to separately estimate spin–lattice and spin–spin relaxation times, T_1 and T_2, respectively, for both sites according to the above procedure [16].

Figure 5 presents the relaxation spectra of polarons and fullerene anion radicals photoinduced in the bulk PHT–PCBM heterojunction as functions of the energy of photons and temperature. Note that, for both charge carriers, dependences $T_1(h\nu_{ph})$ show extrema at 2.1 and 3.1 eV; at the same time, T_2 slightly changes with the energy of photons (Fig. 5a). The initial PHT–PCBM composite is characterized by a monotonic change in relaxation times T_1 and T_2 with temperature for photoinduced charges (Fig. 5b). Because of thermal annealing of the sample, spin–lattice relaxation time T_1 of polarons decreases, while T_1 of fullerene anion radicals increases. Moreover, this modification is the cause of nonmonotonic dependence $T_2(T)$ for both charge carriers in the central region of the temperature interval. This behavior suggests that the mechanism and rate of electron relaxation in the system are dependent on the energy of initiating radiation and are controlled by the conformation of the bulk polymer–fullerene heterojunction. This reasoning confirms the above assumption of the formation of clusters with different structural ordering and band gaps in a given composite.

The bulk heterojunction can involve various dynamic processes, including diffusion of polarons along and between polymer chains with corresponding diffusion coefficients D_{1D} and D_{3D} as well as rotational diffusion of fullerene anion radicals about the selected molecular axis, D_{rot}. The above processes generate additional magnetic fields at the localization sites of electrons and nuclear spins that, in turn, accelerate the electron relaxation of spin reservoirs. Since this relaxation is primarily controlled by the dipole–dipole interaction between electron spins [33], dynamic parameters of both charge carriers can be estimated

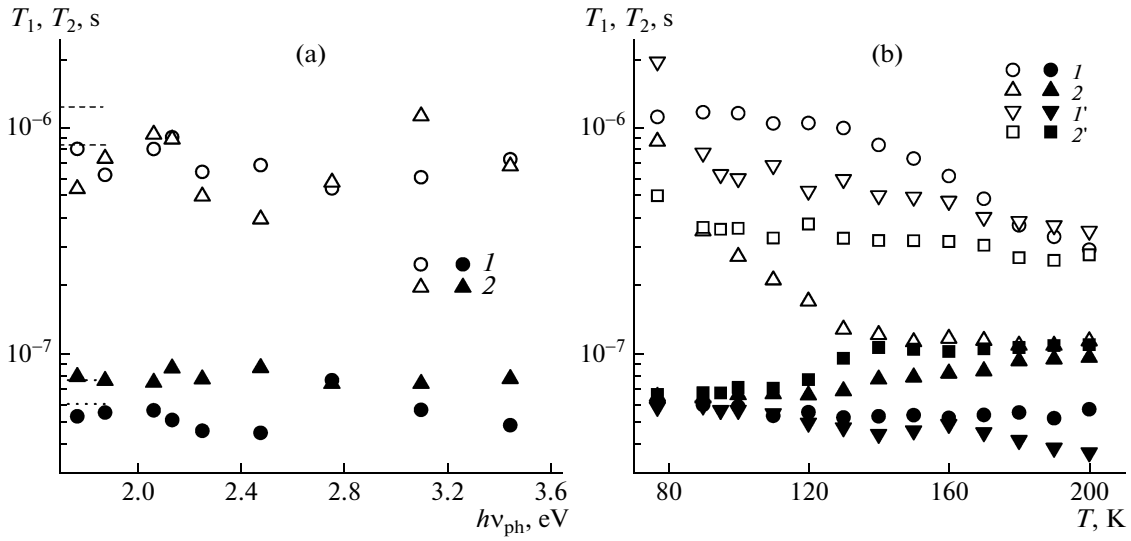

Fig. 5. (a) (Open circles) Spin–lattice relaxation time T_1 and (closed circles) spin–spin relaxation time T_2 of polarons (*1*) $P^{+\bullet}$ and (*2*) fullerene anion radicals $C_{60}^{-\bullet}$ plotted against incident-photon energy $h\nu_{ph}$ during continuous illumination of the PHT–PCBM composite at 77 K. The relaxation time estimated during continuous white light illumination is indicated with fragments of dashed and dotted lines, respectively. (b) Temperature dependences of relaxation times (open circles) T_1 and (closed circles) T_2 for charge carriers (*1*, *1*') $P^{+\bullet}$ and (*2*, *2*') $C_{60}^{-\bullet}$ photoinduced by white light in the (*1*, *2*) initial and (*1*', *2*') annealed samples after annealing for 1 h at 413 K.

from the following equations for magnetic resonance [34]:

$$T_1^{-1}(\omega_e) = \langle\omega^2\rangle\left[2J(\omega_e) + 8J(2\omega_e)\right] \quad (11)$$

$$T_2^{-1}(\omega_e) = \langle\omega^2\rangle\left[3J(0) + 5J(\omega_e) + 2J(2\omega_e)\right], \quad (12)$$

where ω_e is the resonance angular frequency of electron spin precession; $\langle\omega^2\rangle = 1/10\gamma_e^4\hbar^2 S(S+1)n\Sigma_{ij}$ is the constant of dipole–dipole interaction for the powder sample; n is the number of polarons per monomer unit; Σ_{ij} is the lattice sum; $J(\omega_e) = (2D'_{1D}\omega_e)^{-1/2}$ (at $D'_{1D} \gg \omega_e \gg D_{3D}$); $J(0) = (2D'_{1D}D_{3D})^{-1/2}$ (at $D_{3D} \gg \omega_e$) is the spectral density function for quasi-one-dimensional diffusion of a polaron; $D'_{1D} = 4D_{1D}/L^2$ (L is the delocalization factor of polaron spin density on approximately five monomer units in PHT [6, 32]); and $J(\omega_e) = \tau_c/(1 + \tau_c^2\omega_e^2)$ is the spectral density function for the rotational diffusion of fullerene with correlation time τ_c. For both charge carriers in the PHT–PCBM composite, dynamic parameters calculated through Eqs. (11) and (12) are shown in Fig. 6 as functions of the energy of photons and temperature. Analysis of the above data shows that both photoinduced charge carriers in the system under study are characterized by nonmonotonic dependences of coefficients D_{1D}, D_{3D}, and D_{rot} on $h\nu_{ph}$. These dependences show extrema in the same regions as the above extrema for the LEPR linewidth. This result lends additional support for the existence of clusters with different ordering and susceptibility toward photons of the relevant optical interval in the polymer–fullerene composite. For polarons photoinduced in the PHT–PCBM system, quasi-one-dimensional diffusion $D_{1D}(T)$ dramatically decreases with temperature, in contrast to changes in $D_{1D}(T)$ in the poly(3-dodecylthiophene)–PCBM system [10–12, 35]. This behavior can be provided, for example, by a stronger interaction of polarons with lattice phonons in the matrix under study. This interaction should lead to the following dependence of the diffusion rate of a polaron on optical-phonon energy E_{ph} and lattice temperature [36]:

$$D_{1D}(T) = D_{1D}^0 T^2\left[\sinh\left(\frac{E_{ph}}{k_B T}\right) - 1\right] \quad (13)$$

As follows from Fig. 6b, experimental dependences $D_{1D}(T)$ for initial and annealed PHT–PCBM samples are well described by Eq. (13) with E_{ph}, which are listed in the table. The calculated energies of lattice phonons lie near the corresponding values estimated for poly(3-octylthiophene) [17] and some other conjugated polymers [22, 37, 38]. In addition, they approach activation energy E_a for the mobility of polarons in PHT [39] but are lower than E_a for the diffusion of polarons in poly(3-methylthiophene) [40] and in the poly(3-octylthiophene)–PCBM system [41].

Rotational diffusion of fullerenes can be interpreted in terms of the Elliott model for the hops of charge carriers over energy barrier E_b [42]. This model

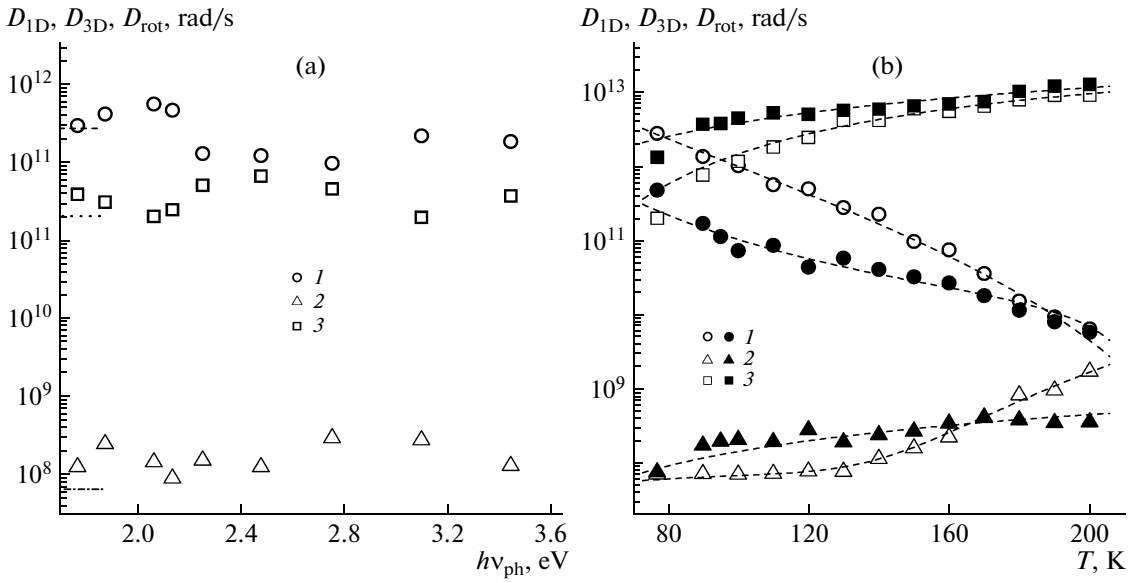

Fig. 6. (a) Coefficients of diffusion of the hopping of polarons $P^{+\bullet}$ (*1*) along polymer chains, D_{1D}, and (*2*) between polymer chains, D_{3D}, and (*3*) coefficient of rotational diffusion of anion radicals $C_{60}^{-\bullet}$ with respect to the main axes, D_{rot}, photoinduced in the PHT–PCBM composite at 77 K plotted against photon energy $h\nu_{ph}$. The same parameters estimated during continuous illumination with white light are shown as fragments of dashed, dotted, and dash–dotted lines, respectively. (b) Temperature dependences of coefficients (*1*) D_{1D}, (*2*) D_{3D}), and (*3*) D_{rot} for charge carriers $P^{+\bullet}$ and $C_{60}^{-\bullet}$ photoinduced by white light in the (open circles) initial and annealed (closed circles) samples for the PHT–PCBM composite after annealing for 1 h at 413 K. Dashed lines show the dependences calculated through Eqs. (13) and (14) with the use of corresponding lattice-phonon energies E_{ph} and activation energy E_b.

predicts frequency and temperature dependence of the diffusion of charge carriers as

$$D_{rot}(\omega_e T) = D_{rot}^0 T^2 \omega_e^s \exp\left(\frac{E_b}{k_B T}\right), \qquad (14)$$

where $s = 1 - \alpha k_B T/E_b$ and α is a constant. For activation of rotational diffusion of fullerene in the initial and annealed samples, the calculated E_b values are summarized in the table. As follows from Fig. 6b, the dependences calculated through Eq. (14) for tabulated E_b values fairly approximate the experimental data. For fullerene, E_b values are appreciably lower than the corresponding activation rotational energy of fullerene in more crystalline compounds [43, 44]; however, they approach E_b for the rotation of fullerenes in the triphenylamine complex [45].

After comparison of the data on spin dynamics for the bulk poly(3-dodecylthiophene)–PBEMA heterojunction [10–12, 35] and data presented in this study, it may be concluded that the rotation rate of fullerene in poly(3-alkylthiophene) decreases by several orders of magnitude with an increase in the length of the alkyl substituent, i.e., on passage from poly(3-hexylthiophene) to poly(3-dodecylthiophene). For the PHT–PCBM composite, the annealing decreases both the anisotropy of diffusion of polarons and E_{ph} and E_b (table). This result verifies that, because of annealing, the degree of crystallinity and the dimension of the system increase. During annealing of the composite, fullerene molecules incorporated into a comparatively amorphous polymer matrix become more mobile and accumulate into fullerene clusters. As a result, in the annealed composite, crystalline polymer and fullerene clusters are formed; finally, the electron transport characteristics of solar cells with bulk heterojunctions improve.

CONCLUSIONS

In the PHT–PCBM composite, illumination leads to the formation of two photoinduced paramagnetic sites with well-resolved EPR spectra, namely, positively charged polaron $P^{+\bullet}$ on the polymer chain and negatively charged fullerene anion radical $C_{60}^{-\bullet}$ located between polymer chains. The two radicals are quickly spaced owing to the high mobility of the polaron; as a result, the probability of their recombination decreases. The LEPR signals from these sites are differently saturated under the action of a microwave field, a circumstance that makes it possible to separately estimate the relaxation parameters for each of the charge carriers. Analysis of the dependences of the main magnetic, relaxation, and dynamic parameters of polarons $P^{+\bullet}$ and fullerene anion radicals $C_{60}^{-\bullet}$ on the energy of excitation photons at 1.7–3.4 eV shows that

they nonmonotonically change as a function of $h\nu_{ph}$ and pass extrema at 2.0 and 3.1 eV. The probability of recombination of such charge carriers follows the activation law and is controlled by the energy of excitation optical photons. Analysis of the dependences of spin susceptibility on the energy of photons and temperature makes it possible to conclude that the number of photoexcited polarons in the PHT–PCBM composite exceeds the number of fullerene anion radicals over the entire temperature interval; during heating, the difference between the concentrations of $P^{+\bullet}$ and $C_{60}^{-\bullet}$ decrease. For a polaron and a fullerene anion radical, the temperature dependences of spin–lattice and spin–spin relaxation times, T_1 and T_2, respectively, are obtained. With the use of this evidence, the diffusion coefficients for the translational motion of polarons along the polymer chain, D_{1D}; for the translational motion of polarons between polymer chains, D_{3D}; and for rotational diffusion of fullerenes, D_{rot}, are found. Owing to the annealing of the PHT–PCBM composite, the anisotropy of diffusion of polarons decreases along with the activation energy of translational and rotational diffusion of charge carriers. This evidence verifies that, because of annealing of the PHT–PCBM composite, the degree of crystallinity and dimension of the system increase.

ACKNOWLEDGMENTS

We would like to thank V.A. Smirnov for helpful discussion.

REFERENCES

1. *Organic Photovoltaics: Mechanisms, Materials, and Devices (Optical Engineering)*, Ed. by S.-S. Sun and N. S. Sariciftci (CRC, Boca Raton, 2005).
2. Z. Zhu, D. Muhlbacher, M. Morana, et al., in *High-Efficient Low-Cost Photovoltaics* (Springer, Berlin, 2009), Vol. 13, p. 195.
3. S. Gunes, H. Neugebauer, and N. S. Sariciftci, Chem. Rev. **107**, 1324 (2007).
4. *Handbook of Conducting Polymers*, Ed. by T. E. Scotheim and J. R. Reynolds (CRC, Boca Raton, 2007).
5. V. Dyakonov, G. Zoriniants, M. Scharber, et al., Phys. Rev. B: Condens. Matter **59**, 8019 (1999).
6. M. Westerling, R. Osterbacka, and H. Stubb, Phys. Rev. B: Condens. Matter **66**, 165220 (2002).
7. *Organic Photovoltaic: Concepts and Realization*, Ed. by C. Brabec, V. Dyakonov, J. Parisi, and N. S. Sariciftci (Springer, Berlin, 2003).
8. K. Marumoto, Y. Muramatsu, and S. Kuroda, Appl. Phys. Lett. **84**, 1317 (2004).
9. S. Sensfuss, A. Konkin, H.-K. Roth, et al., Synth. Met. **137**, 1433 (2003).
10. V. I. Krinichnyi, Khim. Vys. Energ. **42**, 73 (2008).
11. V. I. Krinichnyi, Acta Mater. **56**, 1427 (2008).
12. V. I. Krinichnyi, Sol. Energy Mater. Sol. Cells **92**, 942 (2008).
13. V. I. Krinichnyi, P. A. Troshin, and N. N. Denisov, J. Chem. Phys. **128**, 164715 (2008).
14. V. I. Krinichnyi, P. A. Troshin, and N. N. Denisov, Acta Mater. **56**, 3982 (2008).
15. A. Pivrikas, N. S. Sariciftci, G. Juska, and R. Osterbacka, Prog. Photovoltaics: Res. Appl. **15**, 677 (2007).
16. C. Poole, *Electron Spin Resonance: A Comprehensive Treatise on Experimental Techniques* (Wiley, New York, 1967; Mir, Moscow, 1970).
17. V. I. Krinichnyi and H.-K. Roth, Appl. Magn. Reson. **26**, 395 (2004).
18. S. S. Eaton and G. R. Eaton, Appl. Magn. Reson. **11**, 155 (1996).
19. E. Tosatti, N. Manini, and O. Gunnarsson, Phys. Rev. B: Condens. Matter **54**, 17184 (1996).
20. W. Bietsch, J. Bao, J. Ludecke, and S. Van Smaalen, Chem. Phys. Lett. **324**, 37 (2000).
21. J. De Ceuster, E. Goovaerts, A. Bouwen, et al., Phys. Rev. B: Condens. Matter **64**, 195206–1 (2001).
22. V. I. Krinichnyi, Synth. Met. **108**, 173 (2000).
23. J. Nelson, Phys. Rev. B: Condens. Matter **67**, 155209 (2003).
24. E. Houze and M. Nechtschein, Phys. Rev. B: Condens. Matter **53**, 14309 (1996).
25. Y. N. Molin, K. M. Salikhov, and K. I. Zamaraev, *Spin Exchange* (Springer, Berlin, 1980).
26. V. I. Krinichnyi, H.-K. Roth, M. Schrödner, and B. Wessling, Polymer **47**, 7460 (2006).
27. V. I. Krinichnyi, S. V. Tokarev, H.-K. Roth, et al., Synth. Met. **156**, 1368 (2006).
28. M. Al-Ibrahim, H. K. Roth, M. Schroedner, et al., Org. Electron. **6**, 65 (2005).
29. V. I. Krinichnyi, O. Ya. Grinberg, I. B. Nazarova, et al., Izv. Akad. Nauk SSSR, Ser. Khim. **2**, 467 (1985).
30. N. A. Schultz, M. C. Scharber, C. J. Brabec, and N. S. Sariciftci, Phys. Rev. B: Condens. Matter **64**, 245210 (2001).
31. H. Tanaka, N. Hasegawa, T. Sakamoto, et al., Jpn. J. Appl. Phys. **46**, 5187 (2007).
32. F. Devreux, F. Genoud, M. Nechtschein, and B. Villeret, in *Electronic Properties of Conjugated Polymers*, Ed. by H. Kuzmany, M. Mehring, and S. Roth (Springer, Berlin, 1987), p. 270.
33. V. I. Krinichnyi, A. E. Pelekh, L. I. Tkachenko, and G. I. Kozub, Synth. Met. **46**, 1 (1992).
34. A. Carrington and E. McLachlan, *Introduction to Magnetic Resonance. With Applications to Chemistry and Chemical Physics* (Harper and Row, New York, 1967; Mir, Moscow, 1970).
35. V. I. Krinichnyi, H.-K. Roth, S. Sensfuss, et al., Physica. E (Amsterdam) **36**, 98 (2007).
36. S. Kivelson and A. J. Heeger, Synth. Met. **22**, 371 (1988).

37. V. I. Krinichnyi, *2-Mm Wave Band EPR Spectroscopy of Condensed Systems* (CRC, Boca Raton, 1995).
38. V. I. Krinichnyi, in *Advanced ESR Methods in Polymer Research*, Ed. by S. Schlick (Wiley, New York, 2006).
39. Z. Chiguvare and V. Dyakonov, Phys. Rev. B: Condens. Matter **70**, 235207 (2004).
40. S. Tagmouti, A. Outzourhit, A. Oueriagli, et al., Sol. Energy Mater. Sol. Cells **71**, 9 (2002).
41. V. I. Krinichnyi, Y. N. Demianets, and S. A. Mironova, Physica. E (Amsterdam) **40**, 2829 (2008).
42. A. R. Long and N. Balkan, Philos. Mag. B **41**, 287 (1980).
43. *Physics and Chemistry of Fullerenes*, Ed. by P. W. Stephens (World Scientific, Singapore, 1993).
44. C. C. Chancey and M. C. M. O'Brein, *The Jahn–Teller Effect in C_{60} and Other Icosahedral Complexes* (Princeton Univ. Press, Princeton, 1997).
45. N. N. Denisov, V. I. Krinichnyi, and V. A. Nadtochenko, Khim. Fiz. **17**, 1405 (1998).